

Supporting Information

Zhou et al. 10.1073/pnas.1308419110

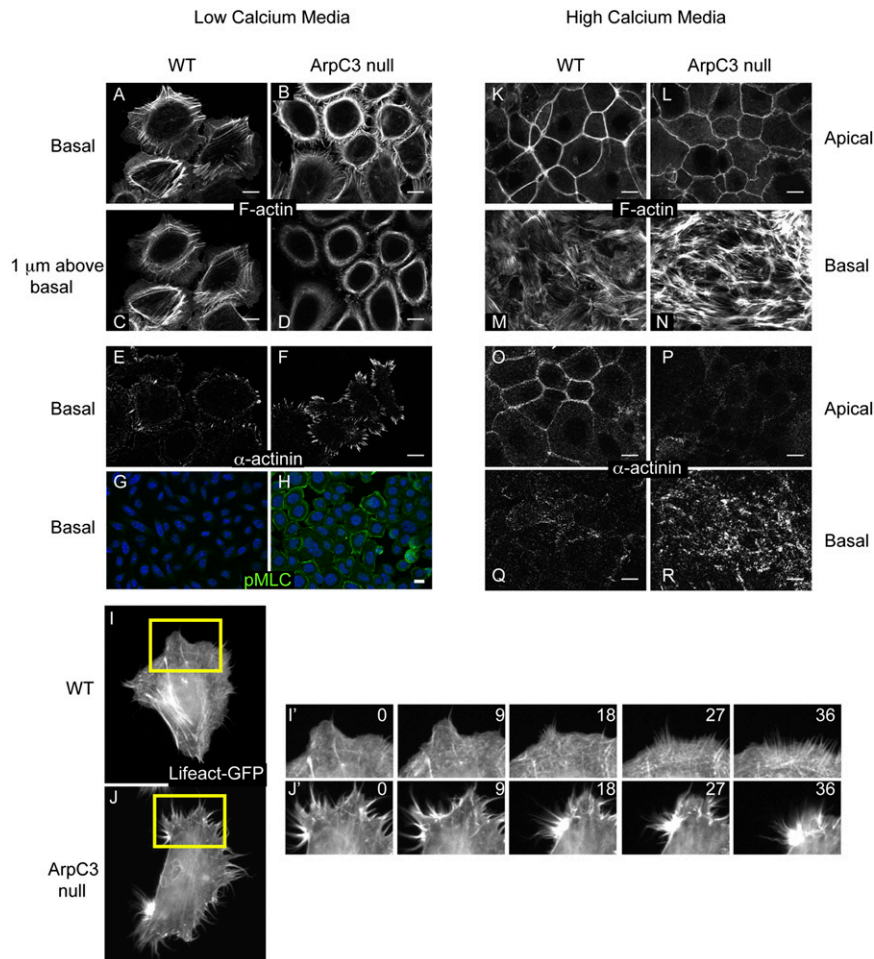


Fig. S1. Changes in F-actin organization in ArpC3-null keratinocytes. (A–D) Rhodamine red-X–phalloidin staining of F-actin in WT and ArpC3-null keratinocytes grown in low-calcium conditions. (E and F) α -Actinin localization at the base of WT and ArpC3-null keratinocytes. (G and H) Localization of phosphomyosin light chain (Thr18/Ser19) in WT and ArpC3-null keratinocytes. (I and J) Images of LifeAct-GFP transfected WT and ArpC3-null cells from which stills of time-lapse movies are drawn. (K–N) Rhodamine red-X–phalloidin staining of F-actin in WT and ArpC3-null keratinocytes grown in high-calcium conditions. Images from the apical and basal sides of cells are shown. (O–R) α -Actinin localization at the base of WT and ArpC3-null keratinocytes. Images from the apical and basal sides of cells are shown. (Scale bars: 10 μ m.)

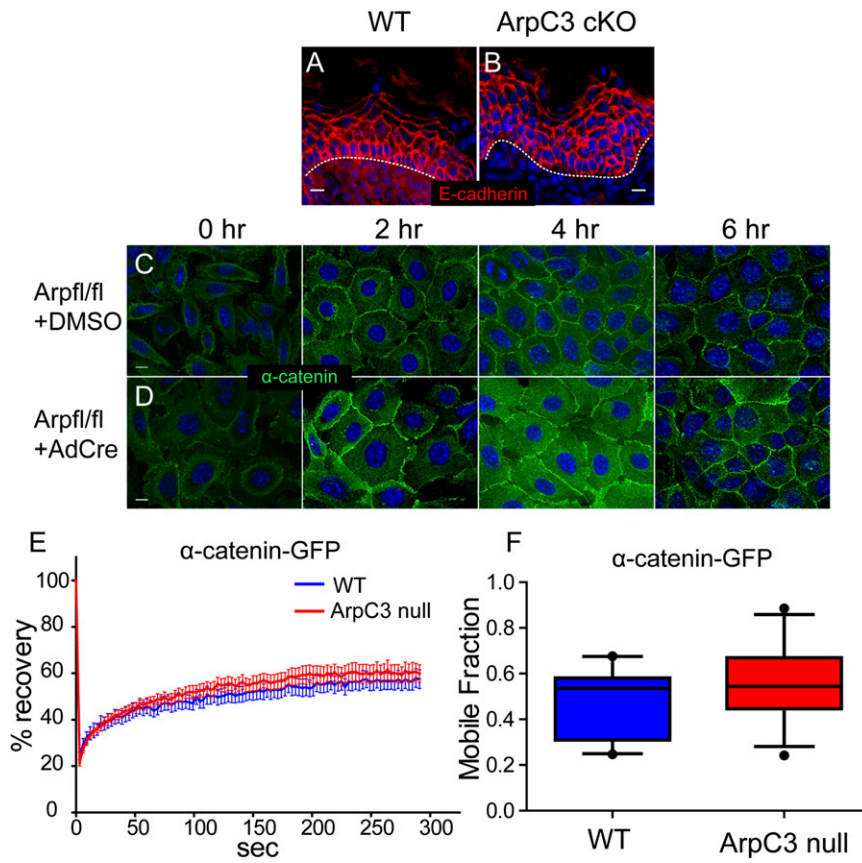


Fig. S2. Lack of notable adherens junction defects upon loss of ArpC3. (A and B) Localization of E-cadherin (red) in WT and ArpC3 conditional knockout (cKO) epidermis. The dashed line indicates the basement membrane. (C and D) Time course of adherens junction assembly upon addition of 1.2 mM calcium to the media. The cortical recruitment of α -catenin is shown over a 6-h experiment. (E) Fluorescence recovery after photobleaching analysis of α -catenin-GFP in WT and ArpC3-null keratinocytes. (F) Quantification of the mobile fraction of α -catenin-GFP in WT and ArpC3-null keratinocytes. Boxes represent 25% to 75%, whiskers represent 5% to 95%.

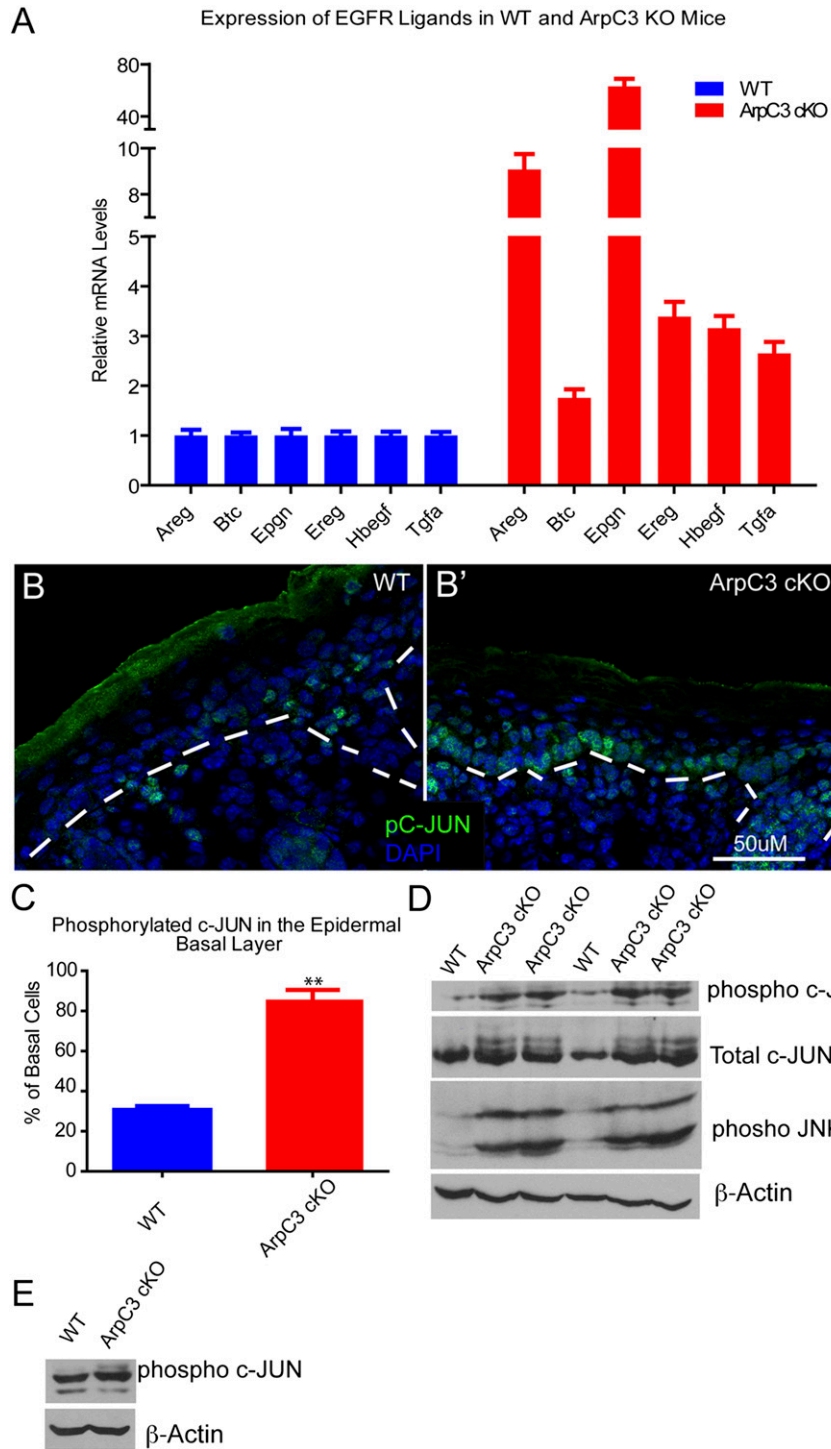


Fig. S3. Changes in EGFR ligand expression and Jun activation in ArpC3 cKO epidermis. (A) quantitative PCR analysis of the expression of six EGFR ligands in two WT and two ArpC3 cKO epidermal preparations (Areg, $P < 0.0001$; Btc, $P = 0.001$; Epgn, $P < 0.0001$; Ereg, $P < 0.0001$; Hbegf, $P < 0.0001$; Tgfa, $P < 0.0001$). (B and B') Immunofluorescence of active phospho c-Jun (green) in WT and ArpC3 cKO epidermis. The dashed line indicates the basement membrane. (C) Quantification of the number of basal cells that are positive for phospho-c-Jun in WT and ArpC3 cKO epidermis ($P = 0.0035$; $n > 300$ cells from each of two independent experiments). (D) Western blot analysis of phospho-c-Jun, total c-Jun, phospho-JNK, and total JNK in WT and ArpC3 cKO epidermal lysates. (E) Western blot analysis of phospho-c-Jun levels in WT and ArpC3-null keratinocytes.

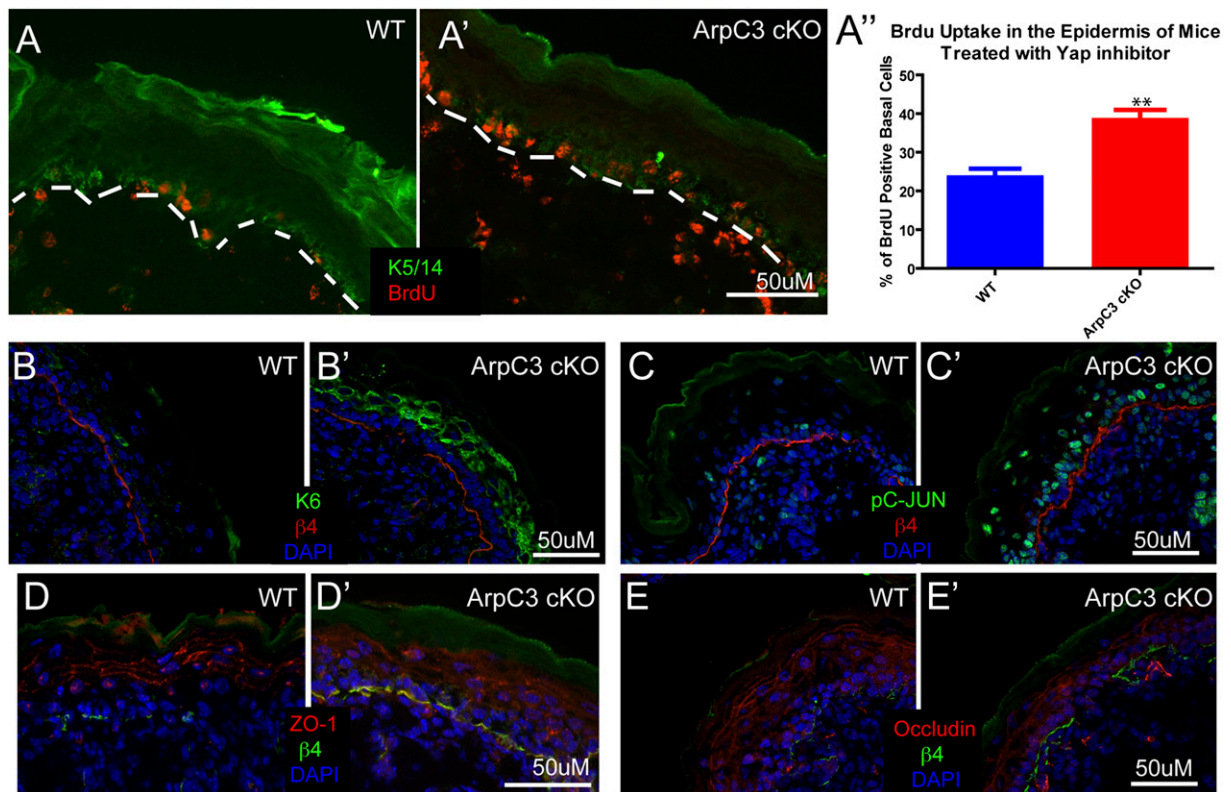


Fig. 54. YAP inhibition does not rescue proliferation, stress, or tight junction defects in ArpC3 cKO epidermis. (A and A') Immunofluorescence and quantification of BrdU incorporation into basal cells of the epidermis in WT and ArpC3 cKO epidermis after treatment with verteporfin ($P < 0.0001$). (B–E) Localization of keratin 6, phospho-c-Jun, and the tight junction proteins ZO-1 and occludin in WT and ArpC3 cKO epidermis treated with verteporfin as indicated.